To be published in:
"ANNALS OF NEW YORK ACADEMY OF SCIENCES"

BNL 26282

CONF-790674--3

DETERMINING BIOLOGICAL FINE STRUCTURE BY DIFFERENTIAL ABSORPTION OF SOFT X-RAYS*

Barbara J. Panessa-Warren
Department of Orthopedic Surgery
State University of New York
Stony Brook, New York 11777

and

John B. Warren
Instrumentation Division
Brookhaven National Laboratory
Upton, New York 11973

June 1979

*This research was partially supported by the U. S. Department of Energy: Contract No. EY-76-C-02-0016.

DETERMINING BIOLOGICAL FINE STRUCTURE BY DIFFERENTIAL ABSORPTION OF SOFT X-RAYS*

Barbara J. Panessa-Warren
Department of Orthopedic Surgery
State University of New York
Stony Brook, New York 11794

and

John B. Warren
Instrumentation Division
Brookhaven National Laboratory
Upton, New York 11973

Morphologically faithful contact replicas have been made of biological specimens placed on photoresist and exposed to ultrasoft X-rays.[1] The copying of the biological fine structure on the photoresist occurs as a result of the differential absorption of soft X-rays by the specimen. Areas of higher atomic number absorb, or stop, the incident X-rays from exposing the underlying photoresist, whereas regions that are composed of low atomic number materials permit the incident X-rays to pass through the specimen exposing the photoresist below. The degree of exposure of the photoresist is a direct function of the chemical (elemental) structure of the specimen, as well as the specimen thickness.[2] This phenomenon is illustrated in Figure 1, which shows a schematic representation of a 100 nm thick plastic embedded section of human nerve placed on top of an equally thick layer of photoresist. In this case the photoresist is polymethylmethacrylate, PMMA. After exposure of the specimen-resist preparation to ultrasoft X-rays, the section is removed and the PMMA developed. A schematic representation of the resultant replica profile shows that in the areas of the section devoid of tissue, their is a maximum exposure or 'etching' of the

*This research was partially supported by the U. S. Department of Energy: Contract No. EY-76-C-02-0016.

photoresist, producing a very deep profile. In areas of the tissue section drawn to represent a dense accumulation of a gold histochemical reaction product within a myelinated nerve fiber (area in black), the soft X-rays have not been able to penetrate the specimen significantly, resulting in the minimal exposure of the photoresist. When the latter region is developed, the replica profile exhibits a height almost equal to the thickness of the resist. For equal section thickness, the greater the difference in the atomic number of adjacent tissue components in the section, the greater the difference of the height of those components in the developed replica. Unfortunately, the fidelity and clarity of the contact replica not only depends on the differential absorption of the incident X-rays by the specimen, but also is dependent on the specimen density and the characteristics of the X-ray source.[2]

This study demonstrates the use of soft X-ray contact microscopy in examining histochemically treated human tissue embedded in plastic and exposed as unstained thin sections. When our preliminary data revealed that we could clearly image not only the histochemical reaction product, but the unstained biological fine structure of the surrounding tissues, we decided to test our hypothesis further and see if we could image unstained biological molecular aggregates as well. For this part of the investigation, we chose to examine hydrated proteoglycan aggregates. Proteoglycans are an essential component of the organic matrix of cartilage, and play a primary role in the retention and maintenance of extracellular water. To date, studies describing the fine structure of these molecules have been done by imaging these aggregates after treatment with ammonium acetate, cytochrome C, and uranyl acetate.[3,4] To avoid any artifacts due to the introduction of these exogeneous materials, and examine the proteoglycan aggregates in their hydrated, natural configuration, we made contact X-ray images of isolated proteoglycan aggregates in water.

Materials and Methods

Sectioned Preparations

In order to eliminate imaging problems due to variations in specimen thickness, all specimens examined were embedded in plastic and sectioned at 90-110 nm thickness on a diamond knife. Human ligamentum terres was excised and immediately fixed in 3% glutaraldehyde in 0.1 M cacodylate buffer (7.4 pH) for 2 days. The tissue was then histochemically treated with gold chloride using the Ranvier technique.[5] After gold localization, the tissue was impregnated with 50% glycerol, and the surrounding collagen teased away from the nerves. The isolated nerves were then rehydrated, dehydrated in acetone, embedded in plastic (Epon 812) and sectioned. Sections for routine transmission electron microscopy (60-90 nm thick) were stained with aqueous uranyl acetate and lead citrate and examined at 80 keV on a Philips 200 transmission electron microscope.

Light microscope slides of ¼, ½, and 1 μm plastic sections were stained with azure II-methylene blue and were used for orientation purposes. To check the validity of the gold reaction product, similar unstained slide preparations were subjected to X-ray microanalysis. The slides, with sections, were broken and the fragments were attached to a graphite stub with colloidal graphite. The samples were coated with 4-10 nm of carbon in a vacuum evaporator with a rotary tilt stage. X-ray maps of gold M X-ray events (2.148 keV) were made for 250 sec., with a voltage window of 2.08 to 2.23 keV on a Tracor Northern energy dispersive spectrometer. Maps were also made with windows at 1.75 to 2.05 keV and 2.28 - 2.58 keV in order to distinguish between characteristic gold M events and X-ray continuum. Initially, unstained plastic embedded thin sections (90-120 nm thick) were placed on 100 mesh copper grids and the entire grid placed directly on PMMA coated glass chips. We subsequently changed our

procedure and placed the sections directly on silicon dioxide wafers coated with PMMA (Figure 2). Specimens on grids were exposed at the Stanford Synchrotron Radiation Laboratory using broad band radiation (approximately 2-6 nmλ) and 9 - 33 min. exposures. All of the sections placed directly on PMMA coated SiO_2 wafers were exposed at IBM to carbon K_α X-rays (λ = 4.48 nm) at approximately 1 x 10^{-5} Torr for 16, 40, or 50 hr. exposure periods, using a stationary X-ray source.

After exposure the SiO_2 wafers were broken into pieces, each piece having 1 or more sections attached (Figure 3). The sections were removed from the SiO_2 wafers with a mild detergent and distilled water, or with ethanol and water. Sections on grids were simply lifted off the PMMA and the resist checked microscopically for any residual section fragments. In both cases the PMMA was then developed in a 5:1 mixture of isopropanol to methylisobutylketone for periods ranging from 20 to 300 seconds. By developing each specimen for a different period of time, it was possible to examine the variations in the ultrastructural information as a function of development depth.

Molecular Aggregate Preparation

Proteoglycan aggregates were isolated from bovine embryonic rudiments[6] using 4M guanidinium chloride in the presence of protease inhibitors and a cesium chloride density gradient. To prevent any imaging of a suspension buffer, the isolated proteoglycan aggregates were resuspended in water (5 μg/ml) and placed directly on PMMA coated SiO_2 wafers. Before the droplet of resuspended material could evaporate, the residual fluid was drawn-off by capillarity using Whatman #50 filter paper. A second droplet was put on the wafer and the procedure repeated. The wafers were then put into polyethylene containers having a small airspace and stored overnight. X-ray exposures, the removal of the specimen, and development of the resist were done as

previously described. Proteoglycan aggregates, isolated on a sodium chloride density gradient, were also examined.

Scanning Electron Microscopy

The developed pieces of photoresist were attached to aluminum specimen stubs with silver conducting paint and the specimens coated with gold-palladium (AuPd) in a vacuum evaporator at 6×10^{-7} Torr using a rotary tilt stage (coating thickness 5-10 nm). An AMR 1000A SEM, equipped with a lanthanum hexaboride gun, was used for examination of the samples. The choice of accelerating voltages, specimen current and tilt angles varied with each specimen. Most of the high resolution work was done at 20 keV, with 110-125 μAmp emission current and tilt angles of 0°, 30°, and 68°. The lower magnification images were taken at 10 keV, with 50-85 μAmp emission current and tilt angles ranging from 30° to 80°.

Results

Sections that had been placed on copper grids and exposed to soft x-rays using the 4° beam line at the Stanford Synchrotron Research Laboratories, produced questionable replicas. After development of the resist, the copper grid and sections containing tissue could be clearly identified in the replicas at low magnification (Figure 4). However at higher magnifications for every single line that was observed in the original tissue section, several lines appeared at the same site in the replica, suggesting some form of diffraction phenomenon (interaction with the grid), specimen vibration, or a poorly defined incident x-ray beam. Figure 4 shows a replica of tissue within a grid-opening showing a capillary in cross section. The nucleus of the endothelial cell (N) and associated cytoplasm are apparent in the replica. At a higher magnification (Figure 5) it is evident that the knife mark, which in the original section consisted of only one line, was replicated in the photoresist

as several distinct ridges (black arrows). The same ridges are apparent at the edge of the copper grid. To eliminate the possibility that the copper grid had produced this type of false replication, due to vibration or detachment of the grid from the PMMA, we placed sections directly on the photoresist. To eliminate the uncertainty about the uniformity and collimation of the X-ray beam, we exposed our specimens to carbon K_α X-rays produced from a stationary X-ray source.

Initial X-ray microanalytical studies to check the accuracy of the gold histochemical procedure revealed that the gold reaction product was selectively localized within the axons of the myelinated nerve fibers. Off-peak X-ray maps showed a sparse, but uniform, distribution of background X-ray events over the entire field of view with no clusters of recorded X-ray events related to the tissue components.

Figure 6 shows an X-ray replica of the nerve fiber after 1 minute development. The areas with the greatest height in replica topography (areas labeled G) correspond to the regions of the section originally possessing the gold reaction product. The cells comprising the nerve fasicle (white arrows) surround the "gold replica" regions. The cell outlines are only vaguely visible due to underdevelopment of the photoresist (R). Frequently fragments of epon (E) would adhere to the plastic of the photoresist (Figures 6 and 7) and prevent development of the underlying replica. Initially a detergent was used to remove the epon sections, but this was later replaced by an ethanol bath followed by a turbulent water rinse.

Figure 7 shows a slightly overdeveloped (4 minute) replica of the perineurium of the nerve. The replica (R) reveals the outline of a Schwann cell nucleus (N), extensive membranous lamelli and bundles of collagen fibers (black open arrows). When the replica is overdeveloped to this extent, much of the fine detail is lost and the edges of the intracellular structures appear smooth and blurry. After a 5 minute

development (under these conditions), most of the replica has been dissolved away, leaving the underlying substrate (S) exposed (Figure 8). In Figure 8, the only remaining fragments of PMMA are those where gold deposits had been replicated (white arrows) or where the epon of the section (E) had fused to the resist thereby preventing development.

Transmission electron micrographs of the histochemically treated articular nerve (black arrows show periphery of nerve) show dense gold deposits (G) within myelinated (M) nerve fibers and Schwann cells (Sc), unmyelinated axons (A) and collagen fibers are surrounded by a reduced perineurium (Pn) (Figure 9). The X-ray contact replica of an identical section of the nerve (black arrows indicate periphery of nerve) exhibits the same anatomical organization, with perineurium (Pn) surrounding the centrally located axons and gold (G) deposits (Figure 10). The delicacy of the developed replica is apparent by the presence of tears and missing fragments revealing the substrate (S) below. Subsequent replicas were handled more carefully to avoid damaging the photoresist surface during specimen removal and development.

Figure 11 shows a higher magnification of a replica of cross sections of 4 myelinated nerves with gold deposits (G) and the neighboring perineurium with collagen bundles (C) and layers of concentric supportive cells. Occasionally, the nuclei (N) of these cells produce replicas with extensive intranuclear detail, which is not apparent by transmission electron microscopy of the identical uranyl acetate and lead citrate stained sections.

Proteoglycan preparations, whether stained with aqueous uranyl acetate or examined unstained, produced clear replicas. Since development of the resist could not be monitored by light microscopy, due to the small size of the proteoglycan aggregates, the 16 hour exposed resists were developed for 10, 30, 45, 60, 75, and 90 seconds. Initially, no structure was apparent on the wafer, but after 30 minutes

a color difference was apparent in the central region of the wafer. The surface area of this developed region corresponded in size to the X-ray exposure area. When we examined these preparations with the SEM we found that the proteoglycans having additional protein produced replicas of anastomosing globular aggregates (Figure 12). Isolated proteoglycan aggregates from cesium chloride density gradient preparations produced replicas (Figure 13) that closely resemble the published morphology of proteoglycans studied by conventional transmission electron microscopy.[4] At very high magnifications, at 0° tilt, the X-ray contact replica reveals extensive morphological detail of the protein-rich proteoglycan aggregates (Figure 14), suggesting that far more information may be available in the replica than can be imaged using conventional scanning electron microscopy.

Discussion

In summary, we found that ultrasoft X-ray contact microscopy provides a very accurate way to image unstained biological specimens at better than 10 nm spatial resolution. Unstained human tissue prepared without osmication produced replicas revealing extensive intracellular fine structure. Chromatin, nucleoli, collagen fibers, and myelin sheath were readily apparent in the replicas, as were many other intracellular components. Histochemical deposition of gold salts and the surrounding unstained cells and organelles were faithfully rendered in the contact replica, thereby providing a new way of accurately imaging histochemical reaction product and surrounding tissue at the ultrastructural level.

From our experience, it can be suggested that the replica may contain far more detail than is apparent at magnifications of up to 50,000 times. Therefore, the standard scanning electron microscope may not have sufficient resolution to take full advantage of this technique.

By breaking the SiO_2 wafers into several pieces with specimens, it was possible to experimentally choose an optimum development time for each sample studied. Over development resulted in the loss of all cellular detail, with only the regions of the specimen corresponding to the highest atomic number remaining intact. Frequently, in over developed preparations, entire areas of photoresist lifted off the SiO_2 wafer and were lost. Underdevelopment of the replica produced some information about surface detail of the specimen and resulted in the most accurate replication of the highest atomic number constituents of the tissue. Therefore it seems that it is optimum to have 2 replica preparations of the same specimen for comparison of detail, one developed to bring out the structures comprised of low atomic number components, and the other developed to bring out the high atomic number detail.

Imaging of unstained, isolated proteoglycan aggregates using this method was relatively simple and produced images that are similar in confirmation to those reported in the literature using transmission electron microscope methods. Unlike the conventional preparations, however, our samples were examined without the introduction of substances that might alter the specimen. The aggregates were placed on the SiO_2 wafers after resuspension in water, and therefore we feel that our images may represent the configuration of the proteoglycan aggregate in a more natural, hydrated state.

Although the soft X-ray contact micrograph is an image of the atomic number topography of a specimen, we are not able at this time to interpret the proteoglycan micrographs in relation to their chemical structure. Stereopairs of the protein-rich and cleaned proteoglycan aggregates clearly demonstrate a repeating periodicity in the height of the globular subunits. However, unlike the thin sections previously studied with intact proteoglycan aggregates, the possibility exists that these molecules may have sidechains in the Z direction (thickness), as well as the X and Y axis. Since the height of the replicated structure in the photoresist is a function of the specimen density, as well as the atomic number, a sidechain of chondroitin sulfate extending upwards in the Z axis would produce the same type of height differential in the replica as a group of atoms with a high atomic number. In the future, the height effect may be interpretable from analysis of contact replica stereo-images and may be quantified by projections at several replica angles.

At present, soft X-ray contact microscopy offers an exciting means of visualizing stained and unstained biological materials at better than 10 nm resolution. When biological tissues are treated with heavy metal stains, the differential absorption of the incident soft X-rays is enhanced, producing more contrast in the contact replica. When histochemical preparations are examined, both the reaction product and surrounding tissue can be clearly delineated in the contact replica. Biological specimens

may be examined intact, although some difficulties may arise in the interpretation of the resultant x-ray contact micrograph due to the thickness of the specimen. We found that we could put wet specimens on the photoresist and begin the x-ray exposure without having to initially dehydrate the sample. This offers the possibility of exposing specimens in their hydrated state, permitting the examination of delicate samples that otherwise might show alterations in morphology if subjected to solvent dehydration or drying. The soft x-ray contact replica reveals ultrastructural anatomical detail, as well as elemental, compositional information about the biological material studied. Therefore, this method of contact microscopy provides a completely new form of ultrastructural analysis for biological research.

Acknowledgement

The authors would like to express their sincere thanks to Mr. Ralph Feder and Dr. David Sayre of IBM Thomas J. Watson Research Center, and Dr. Janos Kirz and Mr. Harvey Rarback of the Department of Physics, State University of New York at Stony Brook for their advice and help. This study could not have been attempted without the assistance and expertise of these scientists.

We would also like to express our gratitude to Dr. Phillip Hoffman of the Department of Orthopedic Surgery, State University of New York at Stony Brook for providing the proteoglycan preparations.

BIBLIOGRAPHY

1. FEDER, R., E. SPILLER, J. TOPALIAN, A. N. BROERS, W. GUDAT, B. J. PANESSA, J. A. ZADUNAISKY, AND J. SEDAT. 1977 Science 197: 259-260.

2. MC GOWAN, W., B. BORWEIN, J. A. MEDEIROS, T. BEVERIDGE, J. D. BROWN, E. SPILLER, R. FEDER, J. TOPALIAN, AND W. GUDAT. 1979 J. Cell Biol. 80: 732-735.

3. ROSENBERG, L., W. HELLMAN, AND A. K. KLEINSCHMIDT. 1970. J. Biol. Chem. 245: 4123-4130.

4. HEINEGÅRD, D., S. LOHMANDER, AND J. THYBERG. 1978. Biochem. J. 175: 913-919.

5. CONN, H. J., M. DARROW, AND V. EMMEL. 1960. Stain Proceedings (Biol. Stain Commission). 2nd ed., William and Wilkins Pub., Baltimore, Md.: 126.

6. OEGEMA, T. R., JR., V. C. HASCALL, AND D. D. DZIEWIATKOWSKI. (1975). J. Biol. Chem. 250: 6151-6159.

FIGURE CAPTIONS

Figure 1. A schematic representation of a plastic embedded cross section of a nerve fascicle, laying on top of a layer of photoresist. The incident soft X-rays (black arrows) are absorbed by dense structures in the section. In less dense areas of the section, the X-rays are transmitted and expose the underlying photoresist. This differential X-ray absorption by the biological specimen results in a selective exposure of the adjacent photoresist. Following development of the resist, a contact replica is in actuality a very accurate atomic number map of the specimen at better than 10 nm resolution (when using PMMA as the photoresist). Therefore, this soft X-ray contact micrograph provides not only ultrastructural morphological information, but information about the chemical architecture of the specimen as well.

Figure 2. This schematic representation shows the steps involved in processing both sectioned and wet molecular biological preparations for soft X-ray contact microscopy.

Figure 3. To insure optimum development of the photoresist, wafers having attached sections, or proteoglycan preparations, were broken into pieces and the individual fragments developed for different time periods.

Figure 4. This X-ray replica of a copper grid with an unstained plastic section, shows a cross section of capillary. The cytoplasm of the endothelial cell and a prominent nucleus (N) are clearly outlined. X-ray: synchrotron, broadband radiation; λ = 1.2 - 6.0 nm; 25 min. exposure; 75 sec. development time. SEM: 20 keV; 80.2° tilt; 50 μAmp emission current.

Figure 5. At higher magnification, there appears to be multiple line replication of the specimen. In the original plastic section, a single knife mark passed diagonally across the section. After development of the PMMA, however, the replica reveals several ridges rather than an accurate copy of the original knife mark. A similar occurrence is seen adjacent to the grid bar (arrows).

Figure 6. This underdeveloped (1 min. development) contact replica (R) of a cross section of human nerve shows poor imaging of the cells surrounding the nerve processes (white arrows), but clearly reveals the regions where gold salts (G) were localized in the original section. Epon (E) has fused to one area of the replica, preventing development and obscuring any cellular detail. X-ray: stationary X-ray source; λ = 4.4 nm; 50 hr. exposure; SEM: 20 keV; 60° tilt; 45 μAmp.

Figure 7. By developing the PMMA for 4 minutes, more cellular detail is apparent. R, replica; E, epon still attached to replica; N, nucleus; arrows point to collagen bundles. X-ray and SEM conditions are the same as Figure 6.

Figure 8. After 5 minutes, the development has progressed to the point where only minimal fragments of the replica (white arrows) can be seen against the bare SiO_2 (S) wafer. The area where a fragment of the original epon embedded section (E) is still attached to the photoresist, illustrates the total depth of the photoresist development. X-ray and SEM conditions were the same as in Figures 6 and 7.

Figure 9. The perineurium (Pn), indicated by black arrows, myelinated processes (M), non-myelinated processes (A), and histochemical deposits of gold (G), within the myelinated axons in this nerve cross section, are readily apparent because the section has been stained with uranyl acetate and lead citrate to increase the specimen contrast for transmission electron microscopy.

Figure 10. An identical section (to Figure 9), imaged by soft X-ray microscopy, reveals extensive ultrastructural details even though the plastic embedded section initially exposed to the carbon K_α X-rays, had no heavy metal stain other than the gold precipitate (G) histochemically localized within the myelinated nerve fibers. The replica is somewhat delicate during and after development and without careful handling will lift-off or break away from the SiO_2 substrate (S). X-ray: stationary X-ray source; λ = 4.4 nm; 16 hr. exposure; 4 min. development. SEM: 20 keV; 60° tilt; 85 μAmp.

Figure 11. A higher magnification of the replica in Figure 10 shows the fine structure of the cells comprising the perineurium (Pn) and the adjacent myelinated nerve fibers with gold deposits (G). Collagen bundles (C) in the perineurium, as well as extensive, ultrastructural detail, are seen in the nuclei (N) of the fibroblasts. X-ray and SEM conditions are the same as Figure 10.

Figure 12. Proteoglycan aggregates, isolated without removing all of the associated protein, appear as globular fragments, or long branching chains, by soft X-ray contact microscopy. X-ray: stationary X-ray source; λ = 4.4 nm; 16 hr. exposure; 1 min. development. SEM: 20 keV; 30° tilt; 100 μAmp.

Figure 13. This X-ray contact replica of a proteoglycan aggregate isolated, using a cesium chloride density gradient, is very similar in morphology to the proteoglycan structure seen by conventional transmission electron microscopy. X-ray: stationary X-ray source; λ = 4.4 nm; 16 hr. exposure; 0.5 min. development. SEM: 20 keV; 60° tilt; 85 μAmp.

Figure 14. At very high magnifications, the contact replicas reveal an elaborate globular configuration of the aggregated proteoglycan molecules (protein not removed). X-ray: stationary X-ray source; λ = 4.4 nm; 16 hr. exposure; 1.5 min. development. SEM: 20 keV; 0° tilt; 120 μAmp.

X-rays
section
resist
replica

FIG. 1

SiO2 wafer
with PMMA
sections placed
on PMMA
TEM
LM
Wet
Preparat
stained
X-ray Exposure
specimen removed
resist developed
specimen coated
with Au Pd
SEM

FIG. 2

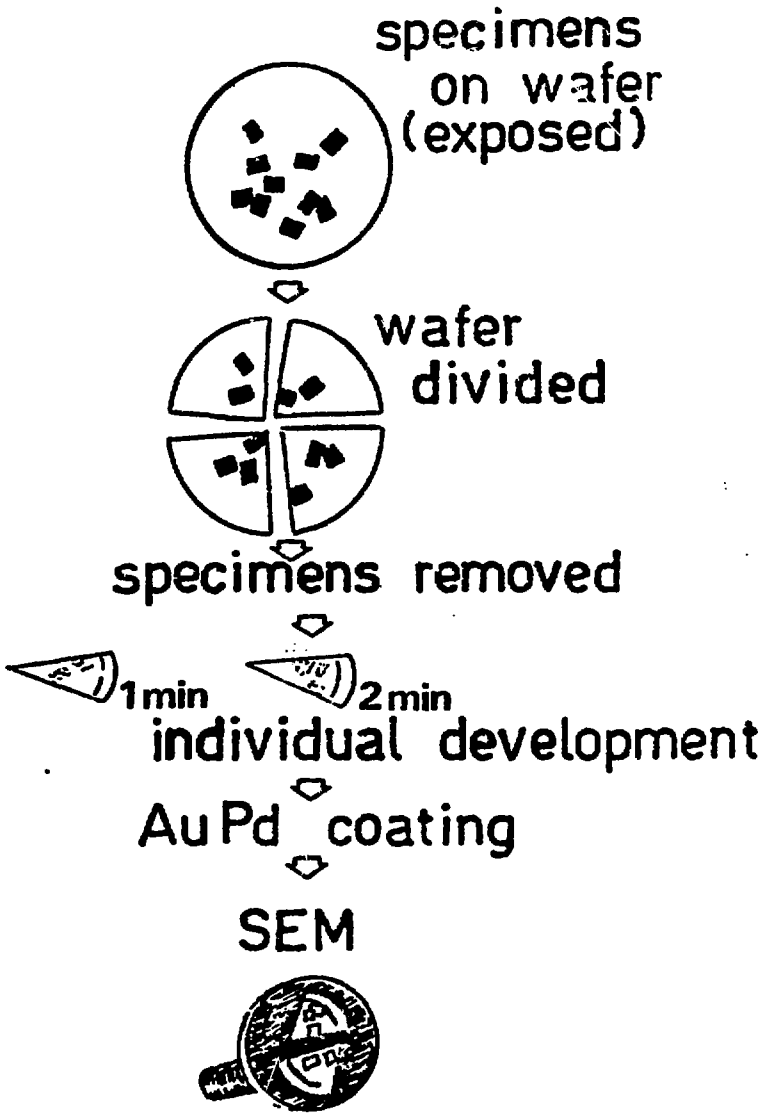
specimens
on wafer
(exposed)
wafer
divided
specimens removed
1min
2min
individual development
AuPd coating
SEM

FIG. 3

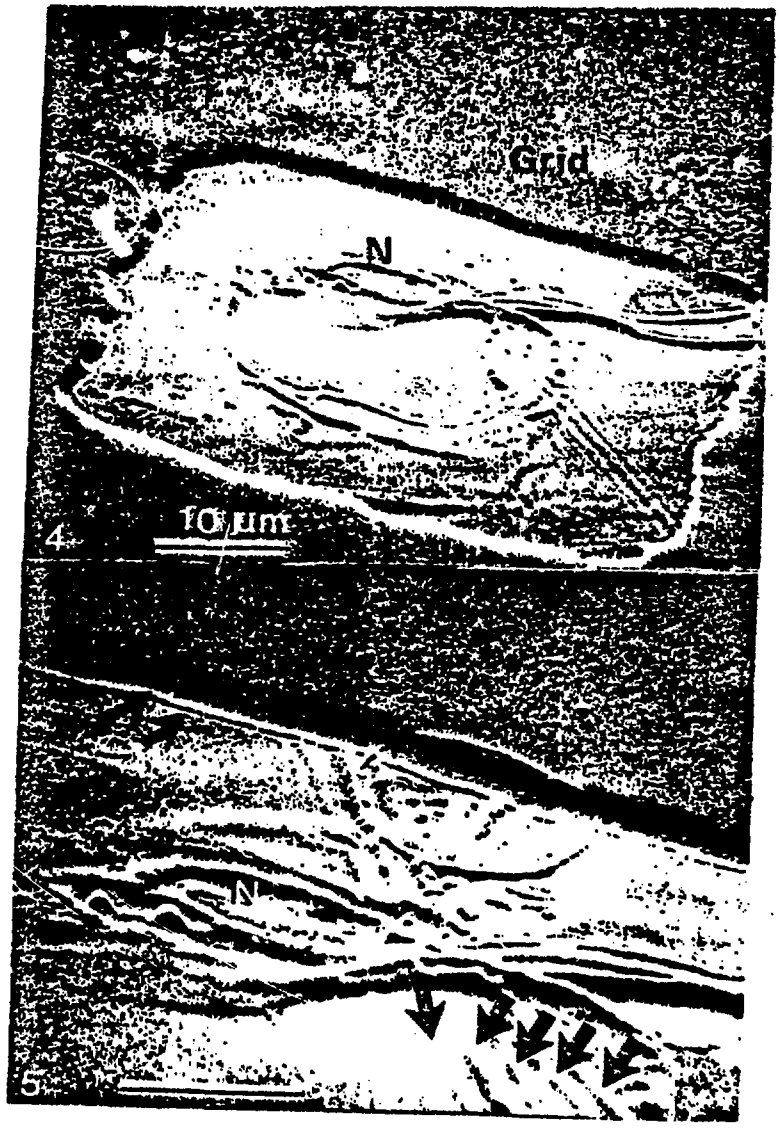
Grid
N
10 µm
4
N
5

R
G
G
G
E
5 µm
6
1 µm
E
N
7
4 min
E
S
5 µm
8
5 min

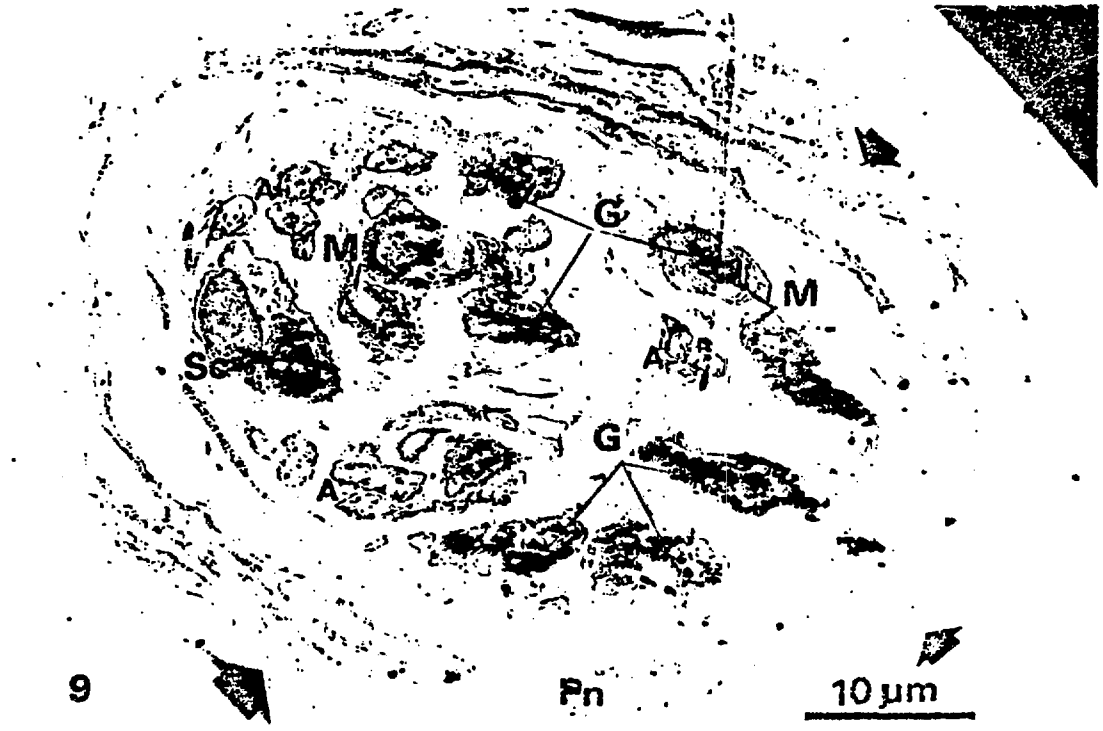
A
M
G
M
Sc
A
G
A
9
Pn
10 µm

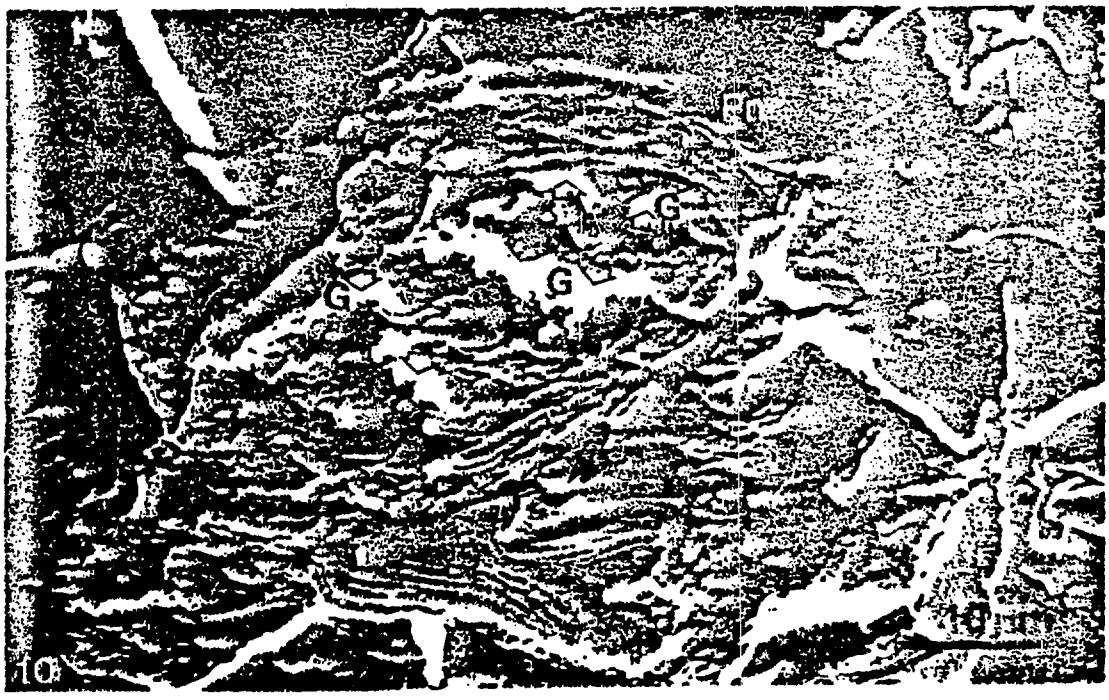
G
G
G
10

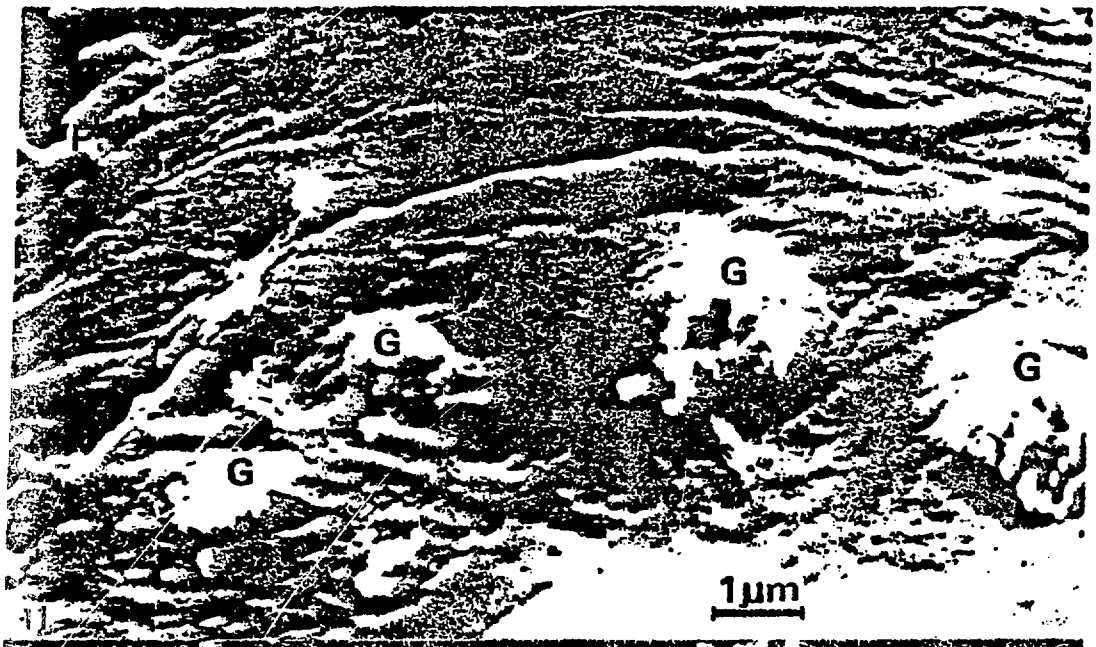
G
G
G
G
1µm


5µm
1µm